

# The processing and characterization of animal-derived bone to yield materials with biomedical applications

## Part 1: Modifiable porous implants from bovine condyle cancellous bone and characterization of bone materials as a function of processing

GLENN S. JOHNSON, MICHAEL R. MUCALO\*

*Chemistry Department, University of Waikato, Private Bag 3105, Hamilton, New Zealand*

MICHEL A. LORIER

*MIRINZ Food Technology and Research Ltd, P.O. Box 617, Hamilton, New Zealand*

*E-mail: m.mucalo@waikato.ac.nz*

A study on the development of a process to form materials suitable for biomedical xenograft implants from bovine cancellous bone is presented. Bone cubes cut from the condyle portion of bovine femurs sourced from abattoir waste were subjected to a defatting and subsequent deproteination procedure to produce shape-modifiable materials in which the biocompatible mineral calcium hydroxycarbonate apatite component was preserved in the original osseous architecture of the bovine bone. Optimum defatting was achieved by (1) thawing of the pre-cut bone cubes in water, (2) pressure cooking at 15 psi in water, (3) soaking in  $0.1 \text{ mol l}^{-1}$  NaOH followed by a thorough rinse under running water, (4) microwave heating of the bone cubes in water, (5) refluxing in methyl acetate and finally (6) removal of internal liquid from the cubes by shaking and then air drying. Subsequent deproteination of the defatted bone cubes was optimally achieved by (1) soaking in 5% sodium hypochlorite solution at ambient temperature using ultrasonication, (2) thorough rinsing of the cubes in water followed by drying. The final product is a defatted/deproteinated, bleached material that can be molded into various shapes for implant use in the body. The bone specimens were characterized by a suite of analytical techniques (i.e. infrared,  $^{31}\text{P}$  and  $^{13}\text{C}$  solid magic-angle spinning (MAS) nuclear magnetic resonance (NMR), X-ray photoelectron spectroscopies, atomic absorption (AA) spectrometry, inductively coupled plasma (ICP) spectrometry, differential scanning calorimetry (DSC), and scanning electron microscopy (SEM)) in order to follow compositional changes during the various stages of processing. In general, bovine condyles proved to be the best source of xenograft materials with condyles from other animal species (i.e. deer, sheep and ostrich) being too small to constitute a utilizable source of cancellous bone. This study shows how value can be added to a hitherto underutilized abattoir by-product by using simple processing techniques.

© 2000 Kluwer Academic Publishers

### 1. Introduction

In the increasingly competitive global market environment, the push towards improved efficiencies and use of resources is a focus of many industries. The New Zealand Meat Industry must contend with the disposal of a large amount of meat by-products that result from the routine slaughter of cattle, sheep and deer. Approximately half of

a large meat animal (e.g. cattle) is eaten in the form of meat and edible offals [1]. Bone comprises about 16–24% of the non-edible by-products of which one sixth is protein when measured on a dry basis. In New Zealand, much of the abattoir bone is rendered into meat and bone meal as well as low value fertilizer for agricultural purposes. There is thus a need to develop products from

\*To whom correspondence should be addressed.

bone with added value. Materials derived from bone have potential for applications in many areas spanning the biomedical, environmental and industrial fields.

Bone sourced from the New Zealand Meat Industry for biomedical purposes has a competitive advantage over other countries in that there is no “controlled herd requirement” as in the European Community which tends to raise the price of raw material from such sources. Secondly, the complete absence of Bovine Spongiform Encephalopathy (BSE)-type ailments in New Zealand livestock adds to this advantage. Thirdly, livestock-derived materials destined for export are strictly regulated by the New Zealand Ministry of Agriculture and Fisheries so allowing a complete audit trail for its processing in New Zealand.

This paper concentrates on the development of a process to form a biomedical implant (xenograft) from bovine cancellous bone. Implant materials cut directly from animal-derived bone are of great value in the biomedical field since they are biocompatible and already possess the correct bony architecture and porosity to allow tissue ingrowth.

There is a well developed literature on the processing, characterization and use of bone-derived materials. The marrow/fat portion of bovine bone gives an antigenic response upon implantation which necessitates its removal. Various removal methods can be used. Akazawa and Kodaira [2] used calcination at 900–1000 °C to prepare ceramic materials from cattle bone apatites. Other less destructive methods may be used which remove fat and organic matter but preserve the bone architecture. For example, Frayssinet *et al.* [3] used CO<sub>2</sub>-supercritical fluid-extracted xenogenic cattle bone in sheep implantation studies. Chappard *et al.* [4] also used mild defatting techniques for preparing bone xenografts and found that wettability was improved with increased defatting.

Bone is a complex material which is sensitive to processing. Changes in bone properties can be followed using various analytical techniques. Vibrational (Raman/IR) analyses of bones are large in number [5–11]. Raman spectroscopy, for instance, has been shown to be useful for characterizing bone mineral and bone mineral-implant interfaces once fluorescing protein has been removed by suitable chemical extraction techniques [8–13]. X-ray diffractometry has often been applied to study the structure of mature bone or nascent bone phases but can offer limited information because of the amorphous nature of bone [14]. Often sintering is needed to effect crystallization to facilitate XRD analysis [15]. Solid state magic-angle angle spinning (MAS) NMR is a better technique for characterizing the partially amorphous bone materials and has been used not only for providing a spectral analysis of bone mineral [16] but also for imaging of bone specimens using <sup>31</sup>P [17].

## 2. Experimental

### 2.1. Source of cancellous bone

The cancellous bone matrix material for implants was sourced from bovine femur condyles in animals slaughtered for human consumption. Bovine bones were obtained directly from local abattoirs. The

carcasses from which the condyles were sourced are believed to be from cattle (breed unknown) between 18 and 30 months old at time of slaughter. The abattoir bone was accorded the same status as meat prepared for export and was thus subject to strict New Zealand Ministry of Agriculture requirements [18]. Ovine bone and cervine bone were obtained from supermarket sheep offcuts and a local deer meat abattoir. Ostrich bone was obtained from a local commercial ostrich farm. Before any processing was initiated, raw bone samples were always stored preserved in a frozen state at –35 °C.

Sectioning of the bone was performed with standard workshop cutting and drilling tools. Each bovine femur has condyles of different sizes, which allows two sections to be removed from the larger and one from the smaller. The femur shaft was removed by cutting as close as possible to the condyle end. Following this, a cut was made through the middle of the end, giving a flat surface to both condyle halves. Following that, two methods for excizing matrix specimens were used, *viz.*, a “borer” method and a “bandsaw” method. In the borer method, a bench press drill with a 25 mm blu-mol borer was used to take cores from the condyle centers. It was necessary to detach the borer from the drill chuck to remove each bone core excised. The ends were then trimmed afterwards to give a core of length 25 mm. In the bandsaw method, successive sections were removed from the condyle surfaces using a bandsaw to obtain 25 mm<sup>3</sup> cubes of cancellous bone. If further cutting of the excised bone cubes was required after the various processing steps (e.g. to monitor the extent of defatting), the cubes were brittle enough to be cut with a hand coping saw.

### 2.2. Solvents and reagents

All solvents and reagents used in the study were utilized as received without further purification. Concentrated bleach solutions as used in deproteinization experiments were industrial grade (25% NaOCl or 50% H<sub>2</sub>O<sub>2</sub>). Pressure cooking of the bones was carried out in potable (tap) water whilst defatting and deproteinization treatments employed distilled water as required. Isopropyl alcohol (IPA) used for solvent-assisted defatting was drum grade whilst all other solvents (e.g. methyl acetate, methanol, ethanol, ethyl acetate) were BDH Anala-R grade. Hydroxyapatite (Ca<sub>10</sub>(PO<sub>4</sub>)<sub>6</sub>(OH)<sub>2</sub>) (Fluka Microselect, >99% purity) and tricalcium phosphate (Ca<sub>3</sub>(PO<sub>4</sub>)<sub>2</sub>) (Fluka Chemica >98% purity) were used as standards for comparison with the bone-derived materials. A sample of Kiel bone was obtained from a private source.

### 2.3. Processing methods

Ultrasonication of specimens was achieved with a NEY ULTRASonic 104X unit. Microwave processing was performed in an NEC N703M 800 watt, 18 liter capacity microwave oven. Pressure-cook processing of bone cubes was carried out in a stainless steel domestic 15 psi pressure cooker with at least 5 cm of water covering the cubes. For other solvent extraction or reflux processing methods carried out at ambient pressures,

stirrer hot plates and a 2 litre round-bottomed flask with a large 55/44 Quickfit neck were employed. Autoclave treatments (when used) of the cubes were achieved by placing them into a wire mesh basket and subjecting the cubes to a 15 min treatment in a Mercer Steam Pressure Autoclave at 100 °C.

Samples of “milled” animal bone from deer (cervine), sheep (ovine) and cattle (bovine) were prepared by crushing cut bone pieces from each animal, crushing in a hydraulic press at 100 psi and pressure cooking in water at 15 psi for 4 h, with a water change every 2 h to remove tissue and fat in the water. The clean bone chips were then dried for 16 h in a 105 °C oven before being ground to a fine powder (particle size < 2 mm) in a hammer mill.

Supercritical CO<sub>2</sub> fluid extraction was carried out using standard apparatus. Bone cubes were held in an extraction vessel between steel grills. After initial exposure to CO<sub>2</sub> gas at cylinder pressure (40–50 bar), the CO<sub>2</sub> gas was then pumped up to high pressure (~150 bar) where it became a supercritical fluid. After passing through heat exchangers for cooling and a Coriolis flow for measurement of flow rate, temperature and density, the supercritical fluid passed through an ice-filled container and then the extraction vessel passing over the bone samples. Extractable organic material was then dissolved and carried off by the fluid which was then subjected to a reduction in pressure after leaving the vessel which returns the CO<sub>2</sub> to gaseous form. The gas passed through a tank of heated water releasing the organic material with the CO<sub>2</sub> gas being subsequently recycled through the system. Two experiments were performed, one on five (steam autoclaved) bone cubes and another on 10 fresh (raw) bone cubes as a comparison. 2 h were required to totally defat the five pressure cooked cubes (processing was stopped when no fat drawoff was detected) and >3 h for the raw bone cubes.

## 2.4. Chemical analyses

Protein analysis was performed using a modified Kjeldahl method [19]. Protein analyzes were usually carried out on samples in the final product batch as well as before and after bleaching steps in the processing in order to determine the level of deproteination.

Elemental analysis of the bone samples was performed by ICP and AA analysis. Two sets of digestions were performed to obtain solution concentrations in the optimum analytical range. Initially 0.200 g of sample was digested in 7 ml of a 2 : 5 HClO<sub>4</sub> : HNO<sub>3</sub> mix. These digests were diluted 125-fold to a volume of 25 ml and used directly for the evaluation of Mg. A 5-fold dilution was made for Ca and P analysis with a 10-fold dilution being made for Na. For analysis of Cd and Pb, 0.500 g of sample was digested in the same acid mix as used in the first digest and the digests were diluted to 5 ml (10-fold dilution factor) and used directly. The 10-fold diluted digest was, however, diluted 5-fold again for the Al, K, Sr and Zn analyses. A standard in-house reference sample was used as a control to check analyses. Cd, Pb and K were analysed on a Perkin Elmer 5100 PC atomic absorption spectrometer whilst Ca, P, Na, Mg, Zn, Al and

Sr were analyzed on a Thermo Jarrell Ash IRIS axial plasma inductively coupled plasma optical emission spectrometer using a plasma argon flow rate of 17 ml/min, nebulizer argon pressure of 32 psi, rf power of 1150 watts and a sampler flow rate of 2.4 ml/min.

## 2.5. Instrumentation

### 2.5.1. FTIR

Infrared spectra of ground bone matrices and milled bone specimens from different animal species were recorded as KBr discs using spectroscopic grade KBr from BDH on a Digilab FTS-40 FTIR spectrometer. Sixteen scans were acquired between 4000 and 400 cm<sup>-1</sup> at 4.0 cm<sup>-1</sup> resolution.

### 2.5.2. Solid state NMR

<sup>31</sup>P and <sup>13</sup>C solid state NMR spectra (of powdered samples packed in 7 mm zirconia rotors spinning at 4.5 KHz) were acquired on a Bruker AC-200 NMR spectrometer, which was equipped with a solid state probe, cross-polarization/MAS accessory and high power decoupling sequence for <sup>31</sup>P. <sup>31</sup>P spectra were referenced to 85% H<sub>3</sub>PO<sub>4</sub> (0 ppm) using KH<sub>2</sub>PO<sub>4</sub> (5.3 ppm) as a secondary external reference and a line broadening factor of 20 Hz in the FTIR process. All <sup>13</sup>C solid state NMR spectra were referenced to tetramethylsilane (0 ppm) using adamantane (38.3 ppm) as a secondary external reference.

### 2.5.3. Electron microscopy

Electron micrographs were performed on thin sections of carbon-coated bone matrix samples mounted on stainless steel stubs with double-sided sticky tape using a Hitachi S4000 SEM. EDX analyses were performed using Kevex Quantex software and a certified hydroxyapatite standard for calcium and phosphorus quantification.

### 2.5.4. X-ray photoelectron spectroscopy (XPS)

XPS analyses were made using a Kratos XSAM X-ray photoelectron spectrometer. Wide scans were acquired over the 0–1100 eV region using non-monochromatized MgK $\alpha$  X-ray radiation of samples affixed to stainless steel sample stubs by means of black carbon-sticky tape. Spectral acquisition step size was 1.00 eV with a dwell time of 600 ms. A 65 eV electron pass energy was used in all wide scans. Narrow scans were performed over the C1s region (275–300 eV) of the spectrum using the same parameters as for the wide scan except that an electron pass energy of 20 eV was used with a 0.15 eV step size and 7000 ms dwell time. Deconvolution of the experimental C1s narrow scan profile was accomplished by use of Shirley baselines and fitting of 75% Gaussian/25% Lorentzian component peaks. Fitted peaks were constrained to a maximum peak width at half height of 2.0 eV. Where possible, binding energy shifts of fitted peaks were corrected for charging by referencing to the position of C1s (284.8.0 eV) from adsorbed (adventitious) hydrocarbons on the samples.

### 2.5.5. Differential scanning calorimetry (DSC)

Qualitative comparisons of fat levels were made using a Perkin Elmer DSC from 30°C up to a maximum temperature of 400°C using a ramp temperature of 15°C/min. Due to the unavailability of a suitable reference material for the bone samples, peak integrals were computed by summation of data points from zero energy to the observed peak maximum on the DSC profile. The number obtained was assumed to be proportional to fat content in the sample and was used to compare the *relative* differences between samples and not as an absolute representation of fat content. The temperature calibration for the DSC instrument was performed with indium metal. Bone matrix material samples (*ca.* 15 mg) were crushed for analysis.

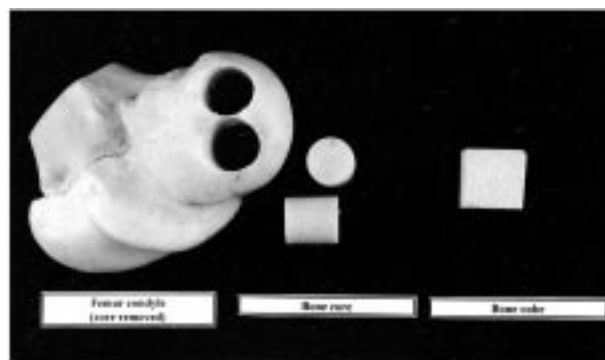
## 3. Results and discussion

### 3.1. Sectioning of cancellous bone matrix to produce bone matrix samples

Fig. 1(a) is a photo of a cut bovine femur condyle showing the source of the bone in this study. Fig. 1(b) shows a photo of a bovine condyle with cylindrical cancellous bone specimens of material removed using a metal blu-mol corer device, as well as cubic specimens. The metal blu-mol borer heated too quickly during cutting so tending to stick during cutting. Cylindrical samples were thus difficult to remove. Attempted cooling of the blu-mol borer simply exacerbated the sticking problem. Moreover such cylindrical cores were usually



(a)



(b)

Figure 1 Photographs of (a) cut bovine femur bone in the condyle region showing the source of cancellous bone cube materials and (b) bovine condyles with cylindrical cancellous bone sections removed from it using a metal blu-mol corer device. These are contrasted with the usual cubes cut from the bovine condyles using a conventional bandsaw.

produced with a very hard and smooth outer surface that subsequently prevented efficient defatting due to the sealing action of friction-induced heat-stimulated denaturing of the bone collagen to sticky glue-like gelatin which hardens on cooling. For this reason, the borer method was abandoned with cubic cuts of bone (prepared by the bandsaw method) being used instead.

Cutting of bone cubes was best achieved using only a very sharp standard workshop bandsaw. Cutting pre-frozen condyles (at -35°C) minimized frictional heating problems. A similar cutting protocol has been followed in earlier studies [10, 20]. It was also important to keep the bone in a frozen state to avoid discoloration which was difficult to remove. During cutting, an effort was made to not produce samples which incorporated harder cortical bone as these tended to frustrate efficient core defatting of the bone cubes. 25 mm<sup>3</sup> cubes were deemed an optimum size for sectioning and processing and for eventual surgical applications. Only bovine bone condyles could meet this criterion. Deer and sheep condyles were too small. Other locations in the bovine skeleton where large volumes of cancellous bone can be harvested were not suitable for processing. The bovine femur head (ball joint), for instance, has a very irregular cross-section which would pose problems with regard to defatting efficiency, mechanical stability and final aesthetic appearance.

Ostrich was the only non-mammal considered as a source of cancellous bone. Suitably large cubes could be cut from the base of the upper large bone of the leg of the bird. These were subjected to similar processing steps as utilized for the bovine-derived cancellous bone (see later).

### 3.2. Defatting of the bovine cancellous bone matrix

#### 3.2.1. Pressure cooking process

Boiling in water under pressure in a conventional pressure cooker was found to be an essential precursor processing step that led to efficient, overall defatting. Vigorous boiling under pressure initiates the denaturing of collagen with the water enhancing physical removal of matter from the pores of the bone matrix by providing a medium for its dispersal. A 6 h pressure cook allowed thorough defatting and retention of the structural integrity of the bone matrix. The pressure cooking was important for removing the bulk of the fat and intertrabecular matter but not all. Subsequent solvent extractions and/or processes such as ultrasonication, microwaving or supercritical extraction methods tended to remove the balance of the fat (see next section).

#### 3.2.2. Defatting using refluxing organic solvents

After pressure cooking of the cubes, refluxing in an organic solvent was necessary for removing residual fat. Initially, IPA was used due to its clinical acceptability and widespread use in surgery for sterilization of medical instruments. However, methyl acetate was preferentially used in this study as (1) fat is highly soluble in this solvent and (2) methyl acetate has a boiling point of

58 °C which is just below the denaturation temperature of type 1 collagen (60–65 °C) [21]. This allows the methyl acetate to extract fat but at the same time prevent the gelatinization side reaction of residual pore-resident collagen during the refluxing which can clog bone pores and restrict defatting of cubes through to the core. Previous workers [8,22] have used chlorinated and hydrazine-based solvents with success as defatting/deproteination agents. These were avoided in the present study for fear of producing biomedical implant materials with unacceptable levels of potentially toxic residues.

### 3.2.3. Ultrasonication

Ultrasonication alone did not result in any significant removal of fat material from the bone cubes (if ultrasonicated in water or IPA). However, when used on samples after pressure cooking, it was highly effective for removing fat traces. For example, pre-processing of the bone cubes by pressure cooking in water (see earlier) gave better results when the cubes were subsequently ultrasonicated for 10 min in IPA than when bone cubes (not pressure cooked) were ultrasonicated in IPA. Ultrasonication must be used with caution, however, as a small amount of damage to the mineral structure of the bone cubes can occur.

### 3.2.4. Microwave processing

Microwaving of the bone cubes in water or organic solvents was a novel defatting method trialled in this study. Bone and fat absorb microwave energy preferentially to other food matter so that meat surrounding bone will be cooked first. The temperature rise of a material subjected to microwave energy is determined by its dielectric loss, specific heat capacity and emissivity as well as the strength of the applied microwave field [23]. These factors thus cause lipids and fats to exhibit a higher temperature rise than water and many solvents. Fat extraction is also extremely rapid compared to conventional methods. Ganzler *et al.* [24] found that the time for extraction of fat from food by microwave extraction was 5 min as opposed to 3 h when soxhlet extraction methods are used. All these studies point to microwaving as being a potentially effective defatting technique for bone.

Raw cancellous bone cubes initially microwaved in water appeared to give rapid defatting with streams of liquefied fat pouring out of the matrix pores and collecting on the top of the solution. Selective heating of the internal bone core was confirmed by measuring the internal core temperature of a cube microwaved in 50 ml of water for 2 min. It was found that while the internal core of the cube had reached 110 °C (measured 10 s after taking out of the microwave), the temperature of the water surrounding the cube was only 80 °C.

There are some caveats, however, when using microwaving as a defatting technique. Cubes microwaved with no prior pressure cooking gave a poorer result. This was manifested by cubes having an apparently well defatted exterior but a poorly defatted core after sectioning. The interior of such cubes tended to be hard, discolored and were strongly retentive of intertrabecular material, which consisted of solidified,

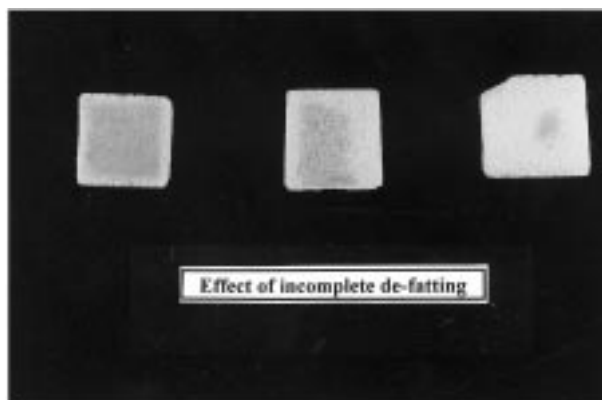


Figure 2 Photo showing the consequences of incomplete defatting procedures in sectioned bone cubes.

gelatinized collagen caused by the intense localized heating of the bone cube that results upon microwaving (see Fig. 2). Microwave processing was more favorable for cubes that had undergone prior pressure cooking in water to remove bulk intertrabecular and other adhering matter.

### 3.2.5. Supercritical fluid extraction

Fig. 3 is a photograph of bovine bone cubes subjected to supercritical CO<sub>2</sub> fluid extraction. It was found that the set of previously pressure-cooked cubes gave the best results in that defatting throughout the entire bone matrix was observed as confirmed by examination of cross-sections of halved cubes. Fresh (not subject to pressure cooking) cubes subjected to the extraction took longer for fat removal and gave poorer results as evidenced by the observation of residual blood streaks and stains on the cubes (see Fig. 3). This was convincing evidence for the need of a pressure cooking step before any other defatting process could be carried out.

### 3.2.6. Development of an optimum defatting procedure

In summary, a procedure for optimizing the defatting of the bone cubes for further processing (*viz.*, deproteination) is as follows:

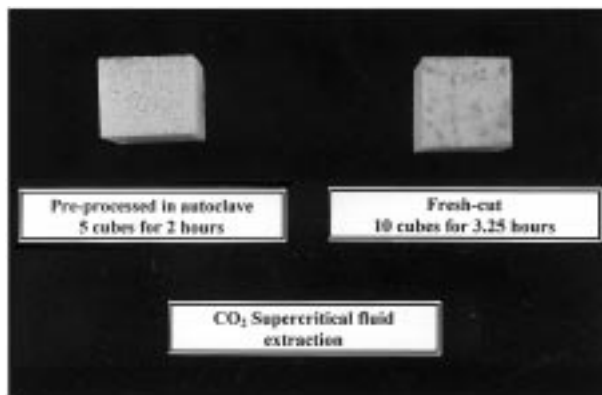


Figure 3 Photograph comparing the results of CO<sub>2</sub> supercritical fluid extraction on cubes which were freshly cut from bovine condyles and on cubes which had been autoclaved for 2 h prior to being subjected to CO<sub>2</sub> supercritical fluid extraction.

- a. Thawing of the precut frozen bovine bone cubes in water for 16 h at 50 °C.
- b. Pressure cooking at 15 psi (103.4 kPa) pressure in potable tap water for 6 h with water changed after 2 and 4 h.
- c. Soaking in 0.1 mol l<sup>-1</sup> NaOH for 16 h, followed by a thorough rinse under running water.
- d. Microwave heating of bone cubes in water on high power (850 W) in a conventional microwave oven for 2 min after reaching the boiling point.
- e. Refluxing in methyl acetate for 1 h with a solvent change after 30 min.
- f. Removal of internal liquid from the pore by vigorous manual shaking (or by compressed air) at the change of each solution or solvent step.
- g. Drying of cubes under ambient laboratory conditions on tissue paper, or direct transferral to the bleaching solution for the subsequent deproteinization step.

### 3.3. Deproteinization of the cancellous bone matrix

#### 3.3.1. A general word on deproteinization agents used

In general, a large number of trials under a variety of conditions involving sodium hypochlorite (commercial bleach) solutions and hydrogen peroxide solutions were carried out for the purpose of deproteinizing or, in other words, removing the bulk of the collagen from the defatted bone cubes. General findings have been described below.

#### 3.3.2. Sodium hypochlorite solutions (NaOCl)

The use of sodium hypochlorite as a deproteinization agent for bone cubes is well established. Cunningham and Balekjian [25] showed that bovine tendon collagen loses 32% of its mass after 12 min immersion in 2.6% NaOCl at 21 °C. Otter *et al.* [26] and Hasegawa *et al.* [27] demonstrated that extended immersion in NaOCl solution resulted in >99% removal of the collagen from a bone matrix. In addition to the well-known oxidizing action of the hypochlorite ion, the relatively high pH of the NaOCl solutions (1% sodium hypochlorite solution has pH ~12.0) effectively denatures the collagen fibers. Other components present in the bone matrices such as residual fat are only slowly oxidized by hypochlorite. For example, Broz *et al.* [28] reported that there was no change to the fat content of cortical bone after 21 days immersion in 5.25% NaOCl at 22 °C with the pH adjusted to 7.0 using HCl.

#### 3.3.3. Hydrogen peroxide solutions

The use of hydrogen peroxide as a deproteinizing agent for bone is not as widespread as in the case of sodium hypochlorite. This bleaching agent was trialled as a possible alternative to hypochlorite solutions so as to eliminate the possibility of chlorinated residues remaining in the final product. Peroxide solutions are significantly more acidic than hypochlorite solutions (3% hydrogen peroxide solution has a pH of *ca.* 3.4).

### 3.4. Effects of bleach on bone matrices

In general, immersion of bone matrix cubes in either of the bleaching agents (sodium hypochlorite or hydrogen peroxide) led to a gradual decoloration of the cubes and the evolution of gas bubbles. The bleaching effectiveness was dependent on a number of variables.

#### 3.4.1. Type of bleach

It was observed that sodium hypochlorite and hydrogen peroxide gave very different results which reflected the differing reactivity of the two bleaching agents towards collagen. The efficiency of decoloration was proportional to the concentration of bleaching agent in solution. Peroxide bleaching solutions had greater penetrability than hypochlorite solutions as they led to very uniform (i.e. defatted to core) bleached bone cubes while bone cubes subjected to hypochlorite treatment tended to exhibit a gradient effect where the surfaces of the cubes were considerably whitened with the core (when the cube was sectioned) being darker colored due to fat staining. Broz *et al.* [28] found that in the case of cortical bone, ashing produced less damage to the cortical bone hierarchical structure than did NaOCl treatment which tended to produce discrete regions of mineralized and chemically altered tissues. In the present study, hypochlorite treatment caused significant weakening of the bovine cancellous bone matrix as shown by SEM (see later).

#### 3.4.2. Volume and strength of bleach

When static soaking of bone cubes in bleaching solution was employed during deproteinization, a ratio of 1 bone cube per 50 ml bleaching solution was used to ensure bleaching activity for several days. In trials where bleaching was conducted in stirred, shaken or ultrasonicated solutions, a greater volume (of bleaching solution) to cube ratio was needed since the mechanical agitation increased the access of the bleaching solution to the cubes thus resulting in an increase in consumption of the hypochlorite.

#### 3.4.3. Presence of fat

Bleaching efficiency was strongly influenced by the defatting history of the bone cubes. Bone cubes still retaining a visible yellowed layer of fat on their surfaces or with internal pores which were still blocked with intertrabecular material tended to exhibit non-uniform surface and core bleaching by either hydrogen peroxide or sodium hypochlorite. The gradient effect exhibited by sodium hypochlorite bleaching solutions was enhanced when higher hypochlorite concentration solutions were employed. Optical microscopic examination of yellowed areas occurring on bone matrix cubes after immersion in sodium hypochlorite solution revealed these areas to be associated with some surface deposited crystalline material, some of which was blocking pores in the bone. These may be due to insoluble sodium salts of long chain fatty acids formed from reaction of the hypochlorite and fat.

#### 3.4.4. Contact conditions

Typically, static soaking experiments involving bone cubes in 1% sodium hypochlorite solution almost invariably gave the distinctive gradient bleaching effect for the cubes. This indicated that the hypochlorite had limited access to internal bone pores. To improve access of the hypochlorite solution to internal bone pores, “shaking” (in which the entire vessel containing solution plus bone cubes) was undertaken. This improved bleaching significantly although full bleaching to the core was only achieved after 13 days in which time the outer bone matrix structure showed evidence of considerable deterioration due to the combined effects of excessive deproteinization and agitation.

In “stirred” solutions where a magnetic stirrer bar (isolated from the bone cubes by placing under an upturned basin) was added to the vessel of soaking bone cubes, much less structural degradation was observed though bleaching to the core of the bone cubes was not achieved. The use of concentrated (25%) sodium hypochlorite merely served to increase the gradient bleaching effect between the surface and the center of the cubes.

The best technique for achieving the criterion of uniform bleaching of the bone cubes through to the core was ultrasonication. Provided the minimum power setting on the ultrasonication apparatus was used, structural degradation was minimized. It was found that one day of ultrasonication in 1% sodium hypochlorite solution gave a decoloring result equivalent to 7 days static soaking of the cube in 1% sodium hypochlorite solution. The ultrasonicated cube, moreover, had much improved color and structural uniformity throughout.

#### 3.4.5. Solution temperature

Broz *et al.* [28] reported that collagen is deproteinized more rapidly in 5.25% sodium hypochlorite solutions at higher temperatures. In the present study, this was confirmed by heating a 1% sodium hypochlorite solution to 40 °C and immersing a bone cube for 5 h. Although the cube was observed to decolorize rapidly, sectioning of the cube revealed that the hypochlorite solution had only penetrated 2 mm below the surface; the internal core remaining a dark creamy color. More uniform deproteinization was obtained in experiments operated at ambient temperature (18–21 °C). Thus all bleaching trials were conducted under ambient conditions. When bleaching for extended periods, the hypochlorite solutions were refreshed regularly to maintain bleaching strength. The frequency of refreshing the solution was determined by a visual assessment of any changes in solution activity (decrease in presence of gas released from cube surfaces, decolorization of the characteristic yellow colored 1% sodium hypochlorite solution). For extended periods (e.g. periods >7 days), refreshing of the solution was less frequent because the levels of collagen in the bone were reduced and thus required less bleach to effect removal.

### 3.5. Development of an optimum deproteinization procedure

In summary, the following optimized procedure was used for deproteinizing the cubes:

- a. Use a volume-to-cube ratio of 50 ml of 5% sodium hypochlorite solution per cube (this strength achieves a compromise between the benefits of using a high strength hypochlorite solution to achieve speedy decolorization and sufficient structure weakening and a low strength solution to avoid excessive degradation of the bone matrix)
- b. Conduct deproteinization at ambient temperature
- c. Ultrasonicate immersed cubes in solution for 24 h on the lowest power setting on an ultrasonic bath
- d. Rinse cubes thoroughly with cold running water, following processing including vigorous manual shaking of the cubes to remove excess liquid from the inner pores
- e. Dry cubes at ambient temperature on tissue paper.

### 3.6. The final product

Fig. 4 is an SEM of a thin section of a successfully defatted and hypochlorite-bleached bovine cancellous bone cube. The macroscopic structural detail of pores is clearly discernible with no evidence of any residual intertrabecular matter arising from incomplete defatting. In addition, the interconnecting porosity desirable for any porous implant is observable. This bone specimen exhibited pore sizes ranging from 50 to 700 μm which encompasses the optimum pore size of 150 μm required for optimum osseointegration [29]. SEM micrographs of the hypochlorite-deproteinized matrix showed some indications of small scale structural deterioration such as chipping at the edge of pores caused by the hypochlorite treatment.

Fig. 5(a) is a photograph of the final product after being shaped by scissors into a spherical shape. This is an embodiment of the product which possesses all the desirable criteria of bone implants processed in this study; *viz.*, uniform (to the core) defatting and deproteinization, aesthetic appeal, and cuttability. The most ideal samples were found to be the condyles cut from bovine species. Ostrich bone cubes (see Fig. 5b) were significantly more open and fragile in nature and had a larger amount of intertrabecular matter present which was difficult to remove without significantly



Figure 4 Scanning electron micrograph of a thin section of successfully defatted/hypochlorite-treated bovine bone matrix.

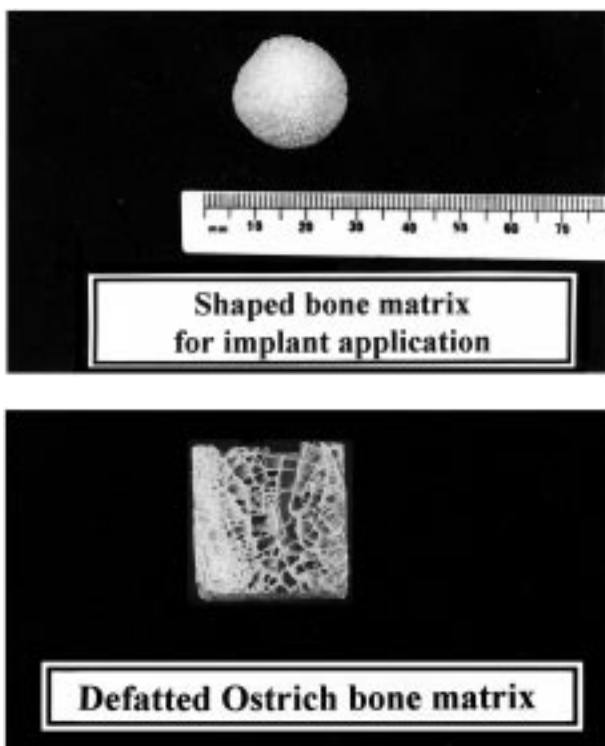


Figure 5 (a) Example of the shaping possible with the bovine matrix after completion of the defatting and deproteination procedures and (b) a cube of processed ostrich bone.

degrading the bone. As a bone matrix implant material, it is too soft and may be more useful if converted into a powder.

#### 4. Application of analytical techniques for studying the bone matrix as a function of processing

##### 4.1. Assessment of defatting

##### 4.1.1. Differential scanning calorimetry as an indicator of residual fat in processed bovine bone cubes

Previous authors have routinely used differential thermal analysis to examine the thermal transitions resulting from the heating of bone material. Two studies [15, 30] have discussed the observations of three distinct thermal transitions in the thermal analysis of bone. These were attributed to (1) desorption of water associated with the bone and the collagen matrix (up to 130 °C, endothermic), (2) combustion of organic material (250–300 °C, exothermic), and (3) crystal phase transitions due to decomposition of carbonates in the crystal lattice (600–900 °C, endothermic).

It was necessary to understand the expected thermal behavior of some of the individual components that make up a bone sample (*viz.*, fat, collagen etc). Fig. 6 is a series of curves comparing the differential thermal analysis profiles measured in this study for fat, isolated collagen, Fluka hydroxyapatite (HAP) and tricalcium phosphate (TCP) samples. As expected, collagen which has water intimately associated with its structure, exhibited a strong endothermic peak centered at 100 °C. TCP and HAP exhibited featureless DSC profiles over the temperature range studied. Pure fat predictably exhibited

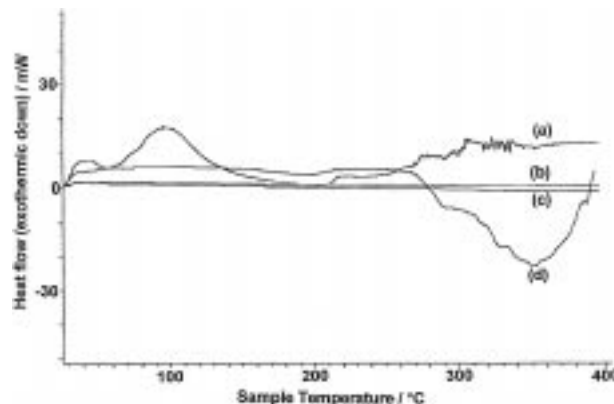


Figure 6 Differential scanning calorimetry (DSC) curves for (a) collagen, (b) Fluka tricalcium phosphate (TCP), (c) Fluka hydroxyapatite (HAP), and (d) beef fat.

a strong exothermic peak between 260 °C and 400 °C due to fat combustion.

Fig. 7 is a series of curves which compare samples of bone from different species studied (*viz.*, bovine, ovine, cervine and ostrich bone). In general, all bone samples gave “endothermic water desorption” stage and the “fat combustion” transition stage peaks within the temperature range studied. However, the intensity of the exothermic fat combustion peak for ostrich bone was markedly higher than for the other animal bone species (see Fig. 7) which indicated there was a larger proportion of organic material present in the ostrich sample. The onset of the fat combustion peak shifted to higher temperatures in all the bone samples relative to pure fat. This indicated that fat interaction with the mineral matrix delayed combustion. In general, the exothermic fat combustion peak exhibited intensity changes depending on the extent of processing of the bone matrix. Defatting efficiencies between bones of different animal species could be semi-quantitatively assessed by comparing the relative intensities of the exothermic fat-combustion thermal transitions between samples. Table I compares integrated peak areas for bovine, cervine, ovine and ostrich bone as well as a bovine bone cube that had been subjected to a deproteination step (see later). The peak positions for samples were consistent to  $\pm 0.5$  °C and the peak areas reproducible to  $\pm 5\%$ . Ostrich bone

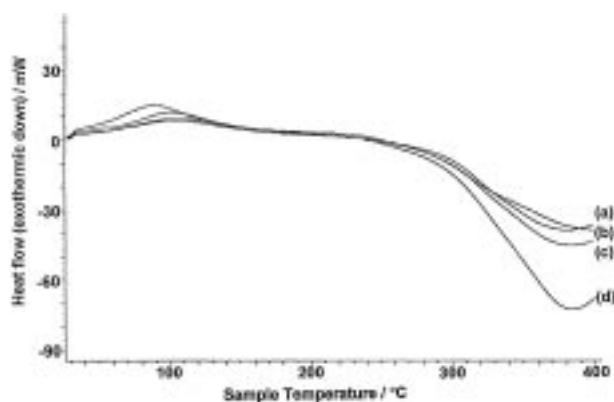


Figure 7 Differential scanning calorimetry (DSC) curves for (a) cervine, (b) bovine, (c) ovine, and (d) ostrich bone specimens.



TABLE I Peak position and integral for the exothermic peak observed in DSC analysis of bone samples from milled animal bones, Kiel bone and bone subjected to deproteination by treatment with sodium hypochlorite

Sample	Peak maximum (°C)	Integral
Kiel bone	380.9	4428
Milled bovine bone	382.7	3455
Milled cervine bone	379.2	2840
Milled ovine bone	395.6	3548
Milled ostrich bone	383.9	4880
Hypochlorite-treated bovine bone matrix	324.4	1419

exhibited the largest peak integral for the fat combustion transition and thus had the largest amount of residual fat remaining in it showing that it did not defat well. Samples of cervine bone showed the best defatting with ovine and bovine bone samples giving intermediate results. The deproteinated bone sample predictably gave lower values for the integrated peak are showing a lower level of fat.

#### 4.1.2. Assessment of deproteination

The level of protein removal by 1% hypochlorite solutions from the cubes was quantitatively assessed by using a modified Kjeldahl method [19]. Duplicate trials showed that 97.5% of collagen is removed by deproteination using 1% sodium hypochlorite solution (i.e. from 16.2 wt% protein before deproteination to 0.4 wt% protein after deproteination).

### 4.2. Elemental, spectroscopic and surface analysis studies of the cancellous bone as a function of processing

#### 4.2.1. Elemental analysis by ICP and AA analytical techniques

Table II is a summary of ICP analytical data for the major elements present in the milled bone powders and a sample of bovine bone matrix at the final stage of its processing (i.e. after deproteination). ‘‘Milled bone powders’’ essentially represent the bone after defatting but before deproteination. Milled bovine bone gave results for the major and trace elements present that were very similar to previous studies on bovine bone [31–33]. All of the milled animal bone species gave molar Ca : P ratios > 1.67 (the ratio expected for stoichiometric hydroxyapatite) thus indicating a calcium hydroxycarbonate apatite where some of the lattice phosphate is replaced by carbonate as expected in natural bone.

Bovine, ovine and cervine bone also gave Na, Mg, Ca and P levels which were broadly similar to each other. Na, Mg, Ca and P levels in ostrich bones, on the other hand, were significantly lower than in bovine, cervine and ovine bones. In the hypochlorite-treated bovine bone matrix, the Na levels were 2–3 times higher than detected in the milled bone powders. It is evident that the use of hypochlorite bleach (sodium hypochlorite) introduces additional sodium into the bone matrix. Trace element levels for the bones for the different animal species (Table III) varied between species. Of significance from a biomedical point of view was the observation that the Cd and Pb levels in samples were all very low. In fact the maximum Pb value of 5 ppm measured (in ostrich bone) was still only 10% of the levels that would commonly be found in mature human bones.

### 4.3. Analysis by FTIR spectroscopy

#### 4.3.1. Defatted bone matrix

FTIR spectroscopy is useful as a qualitative indicator of the level of fat and collagen in the bone after the various processing stages. FTIR spectra of raw bone were not obtained as fresh bone is difficult to sample in practice. Fig. 8 represents spectra of bovine bone as a function of various stages of processing. Fig. 8(a) was the typical spectrum obtained for milled bovine bone. However, the spectral features observed were typical of any bone type regardless of whether it was from sheep, deer, cattle or ostrich. The phosphate fundamental vibrations,  $\nu_3(\text{P-O})$  stretching and  $\nu_4(\text{O-P-O})$  bending modes, were observed at ca.  $1035\text{ cm}^{-1}$  and  $564$  and  $602\text{ cm}^{-1}$  respectively. Collagen-associated bands could be observed in the  $1400\text{--}1700\text{ cm}^{-1}$  region where they overlapped with the IR peaks due to the bending mode of water (ca.  $1640\text{ cm}^{-1}$ ) from entrained moisture and the asymmetric stretch of the  $-\text{CO}_3$  moiety (ca.  $1420\text{--}1450\text{ cm}^{-1}$ ) from the hydroxycarbonate apatite phase in

TABLE II ICP-determined weight% values of the major elements in commercial hydroxyapatite (HAP), tricalcium phosphate (TCP), milled bone from various animals as well as in a bovine bone matrix after hypochlorite treatment

Sample	Na(%)	Mg(%)	Ca(%)	P(%)	Ca : P molar ratio
Fluka HAP	0.007	0.007	40.0	19.0	1.63
Fluka TCP	0.075	0.16	38.1	20.9	1.41
Milled bovine bone	0.50	0.42	25.0	10.5	1.84
Milled cervine bone	0.58	0.39	26.0	10.6	1.90
Milled ovine bone	0.48	0.32	24.0	9.6	1.93
Milled ostrich bone	0.25	0.25	18.4	7.4	1.92
Hypochlorite-treated bovine bone matrix	1.74	0.53	35.9	14.1	1.71

TABLE III Levels (in parts per million (ppm)) of the trace elements present in samples of commercial hydroxyapatite (HAP), tricalcium phosphate (TCP), milled bone from various animals as well as in a bovine bone matrix after hypochlorite treatment. (AA) = Measurement by Atomic Absorption spectrometry, (ICP) = Measurement by Inductively Coupled Plasma Spectrometry

Sample	K (ppm) (AA)	Sr (ppm) (ICP)	Zn (ppm) (ICP)	Cd (ppm) (AA)	Al (ppm) (ICP)	Pb (ppm) (AA)
Fluka HAP	< 10	27	53	1.07	27	0.3
Fluka TCP	30	137	10	0.08	128	< 0.2
Milled bovine bone	80	160	96	< 0.2	60	< 3
Milled cervine bone	120	190	77	< 0.2	< 20	< 3
Milled ovine bone	220	390	104	< 0.2	50	< 3
Milled ostrich bone	70	4900	88	< 0.2	40	5.0
Hypochlorite-treated bovine bone matrix	110	310	168	0.14	57	0.6

the mineral portion of the bone matrix. An additional carbonate-associated IR fundamental ( $\nu_2(\text{C-O})$ ) was observed at  $873\text{ cm}^{-1}$ . In the  $\nu(\text{C-H})$  stretching region ( $2800\text{--}3100\text{ cm}^{-1}$ ), broad weak peaks above  $3000\text{ cm}^{-1}$  are due to C-H vibrations on collagen-associated phenyl group-containing units. Sharper peaks occurring at  $2900\text{ cm}^{-1}$  are due to the aliphatic C-H stretches of residual fat in the bone.

When levels of fat are appreciable in the processed bone materials, the intensity of peaks in the  $\nu(\text{C-H})$  stretching region are enhanced in intensity and an additional peak can be observed at *ca.*  $1744\text{ cm}^{-1}$  which is due to  $\nu(\text{C=O})$  stretching of the carboxyl group in fatty acid molecules. Pressure cooking of the cancellous bone is often not enough to remove surface adsorbed fat. However, subsequent treatment with methyl acetate or IPA serves to wash away these last IR-detectable traces of fat (see Fig. 8(b)).

#### 4.3.2. Deproteinized bone matrix

Deproteinization of the bone by hypochlorite treatment produces a substantial change in IR spectra recorded of the resultant bone matrix (see Fig. 8(c)). Collagen-associated peaks in the  $1400\text{--}1700\text{ cm}^{-1}$  and  $2900\text{--}3100\text{ cm}^{-1}$  regions disappear. Features due to the  $\nu(\text{O-H})$  stretching and  $\nu(\text{H-O-H})$  bending vibrations of water associated with collagen also decrease relative to the  $\nu_3(\text{P-O})$  stretching and  $\nu_4(\text{O-P-O})$  bending modes of the hydroxycarbonate apatite in the bone. The IR spectra show that carbonate is retained by the bone which means that the processing of the bone leaves the mineralized matrix intact. It is possible that even more carbonate is incorporated into the hydroxyapatite lattice during deproteinization as  $\text{CO}_2$  gas liberated under the alkaline conditions in the hypochlorite solution has the propensity to be taken up as carbonate in the hydroxycarbonate apatite lattice [34]. Inspection of the IR spectra of bone

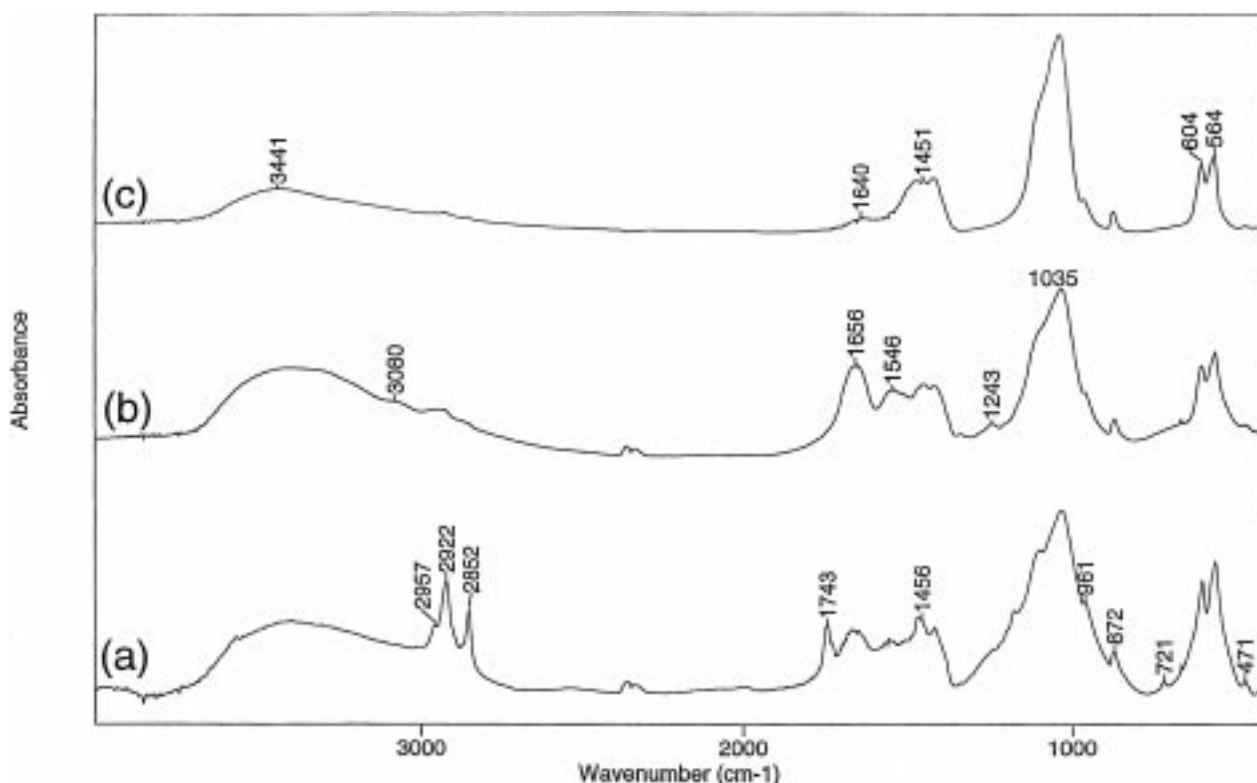


Figure 8 FTIR spectra of bovine bone as a function of processing: (a) after pressure cooking to remove the bulk of the fat and blood, (b) after a solvent wash with IPA to remove residual traces of fat, and (c) after deproteinization of the defatted bone matrix which leads to the final shape-modifiable xenograft product.

before and after deproteination show that an increase in relative intensity for the  $873\text{ cm}^{-1}\nu_2(\text{C-O})$  peak compared to the  $\nu_3(\text{P-O})$  stretching mode peak at  $1030\text{--}1035\text{ cm}^{-1}$  occurs.

#### 4.4. Analysis by solid state NMR ( $^{31}\text{P}$ and $^{13}\text{C}$ )

##### 4.4.1. Defatted bone from different animal species

In general, proton decoupled  $^{31}\text{P}$  solid state MAS NMR spectra of bone is of very limited value as a quick diagnostic technique for following changes in bone composition as a function of processing. This is because all bone specimens examined using standard  $^{31}\text{P}$  solid

state MAS NMR gave single resonances which were invariant in shape between different samples.  $^{13}\text{C}$  solid state MAS NMR spectra, on the other hand, were more useful especially when making comparisons between bone materials sourced from different animal species (i.e. deer, sheep and cattle bone). The  $^{13}\text{C}$  spectra also detected trace fat levels in defatted and deproteinated bone samples not readily detectable by FTIR. Fig. 9(a–f) illustrate  $^{13}\text{C}$  solid state MAS NMR spectra recorded of collagen film, fat extracted from bone, and cervine, bovine, ovine bone and ostrich bone respectively. The  $^{13}\text{C}$  spectra of these naturally-derived materials are typically complex. For instance, comparison of Fig. 9(a) with Fig. 9(c–f) show that the spectra of bone materials consist of superimposed  $^{13}\text{C}$  peaks due to collagen, fat

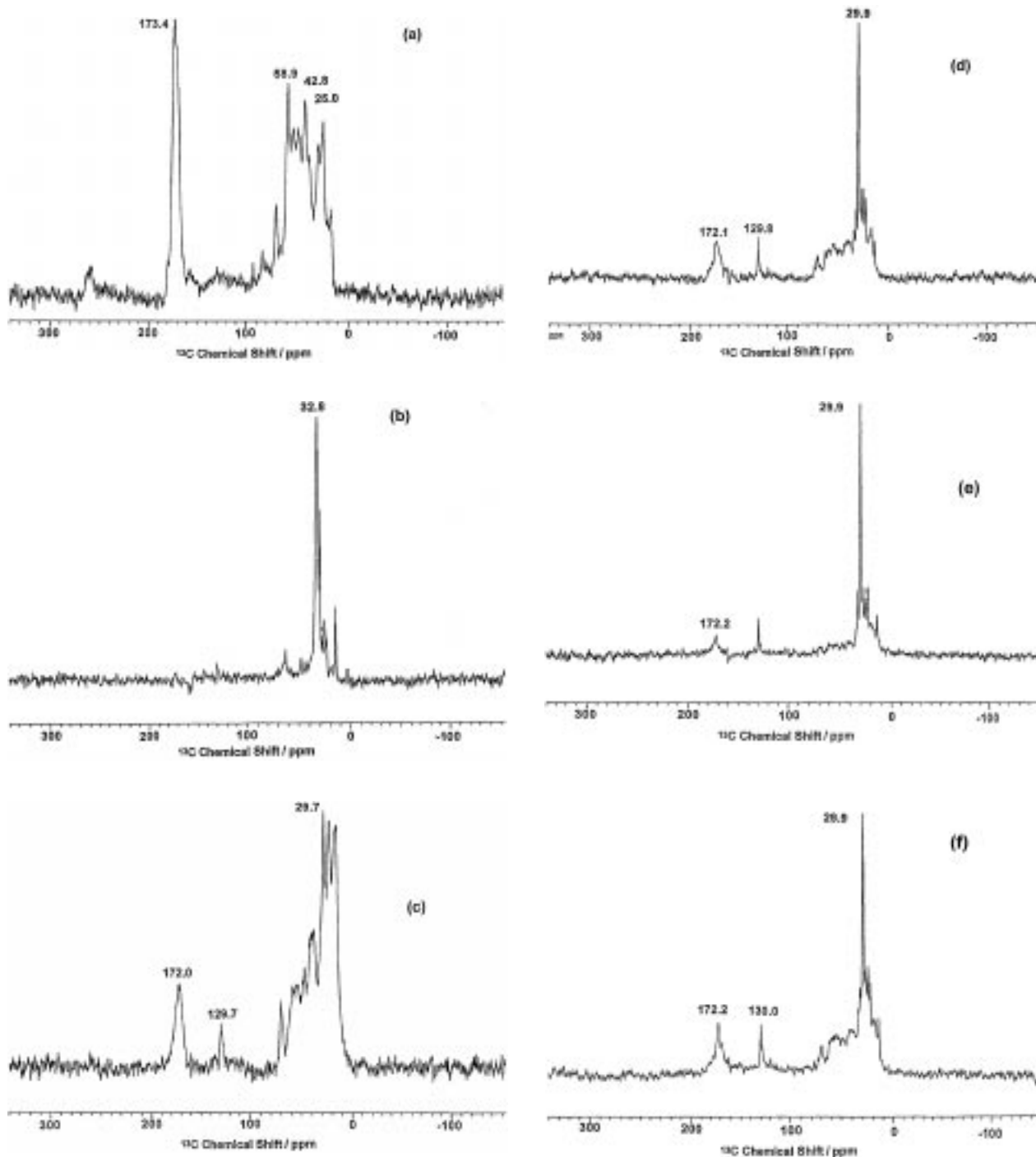


Figure 9 Solid state  $^{13}\text{C}$  MAS NMR spectra of (a) collagen film and (b) bone fat, (c) milled cervine bone and (d) milled bovine bone, (e) milled ovine bone and (f) milled ostrich bone.

and carbonate from the calcium hydroxycarbonate apatite matrix. Due to the degree of overlapping of the peaks from these components, it is especially difficult to separate out the contributions from carbonate (this overlaps with the  $^{13}\text{C}$  resonances for carboxyl-type groups in the collagen) and for fat (these overlap with resonances due to aliphatic-type carbon resonances from the collagen). Inspection of Fig. 9(a) shows that collagen gives a very dominant and characteristic spectrum when it is present. In the bone samples from different species, the relative levels of collagen present in the ground bone samples are significantly different. Ovine bone appears to contain the lowest level of collagen but appears to have a high fat content as evidenced by the observation of the characteristically sharp fat-associated aliphatic  $^{13}\text{C}$  resonance at *ca.* 30 ppm. Ostrich bone gave very similar  $^{13}\text{C}$  spectra to the ovine bone. This is supported by IR spectra which show an elevated level of fat (i.e. detectable  $\nu(\text{C-H})$  and  $\nu(\text{C=O})$  stretching peaks at  $2900\text{--}3000\text{ cm}^{-1}$  and  $1740\text{ cm}^{-1}$  respectively). Both ovine and ostrich bone are characterized by their very fragile and crumbly nature which suggests a low level of collagen in the bone structure.  $^{13}\text{C}$  solid state MAS NMR spectra of cervine bone (Fig. 9(c)) in contrast are dominated by contributions from collagen, although it is obvious from inspection of the 10–40 ppm region that there are also some fat-associated NMR resonances overlapping with the collagen-associated peaks (Fig. 9(a)). Bovine bone had an intermediate level of collagen between cervine and ovine bone. The high levels of

collagen in cervine bone relative to the other animal species studied manifested itself in the visibly harder nature of the material.

#### 4.4.2. Deproteinized bovine bone matrix

Fig. 10(a) is the  $^{13}\text{C}$  solid state MAS NMR of defatted bovine bone deproteinized with hypochlorite. In general, the  $^{13}\text{C}$  spectra mirror IR findings that the bulk of the collagen is removed from the bone with carbonate remaining intact. Indeed, the weak broad peak at 165–170 ppm in Fig. 10(a) is characteristic of a  $^{13}\text{C}$  resonance in a carbonate-type environment [35] and confirmed by recording the  $^{13}\text{C}$  solid state MAS NMR spectrum of a sample of commercial  $\text{CaCO}_3$  (Fig. 10(b)) which shows similar spectral features.  $^{13}\text{C}$  NMR spectra of the hypochlorite-treated bone materials additionally indicated an intense resonance at *ca.* 30 ppm showing surprisingly that there was still some tenaciously held fat on the surface of the bone materials despite the hypochlorite treatment. It is possible that the hydrophobic nature of the bone fat partially precludes its destructive oxidation to gaseous products by aqueous sodium hypochlorite solution and that it may remain as a fatty acid salt on the surfaces of the bone. In summary,  $^{13}\text{C}$  solid state MAS NMR spectroscopy, a relatively underutilized technique in bone characterization studies is thus a more useful indicator of very low collagen and fat levels in the bone samples than is IR spectroscopy.

#### 4.5. Analysis by X-ray photoelectron spectroscopy (XPS)

XPS studies of mineralized bone tissue are few in number being mainly restricted to studies on dental enamel slabs [36, 37]. Landis *et al.* [38] performed an Auger and XPS study on powdered embryonic enamel and young chick bone. Their study established the feasibility of using XPS for qualitative analysis of surface components such as C, O and N. In general, XPS provides information on the first 100 atomic layers of the *surface structure* of bone materials only and is thus not a bulk analysis technique.

Wide scan XPS of bone materials in the present study yielded the typical peaks expected for calcium phosphate-containing materials, *viz.*, Ca 2s, Ca 2p, P 2p, P 2s, O 1s as well as Ca LMM and O KLL Auger peaks. When collagen, fat or carbonate are present in the bone, a significant C 1s peak was also observed. Weak N 1s peaks were observed only when collagen was present in the bone samples.

##### 4.5.1. Referencing and the C 1s narrow scan profile

In general, changes in the bone after processing were only reflected in changes to the C 1s narrow scan peak profiles and thus XPS analyses of the bone samples focused on changes in the C 1s peak (284–296 eV). Narrow scans over the C 1s region of all the samples produced a complex peak shape which was subjected to a mathematical deconvolution process for determining the contributions made by the various carbon-containing components in the samples. A problem encountered with analyzing the C 1s profile was referencing for deducing

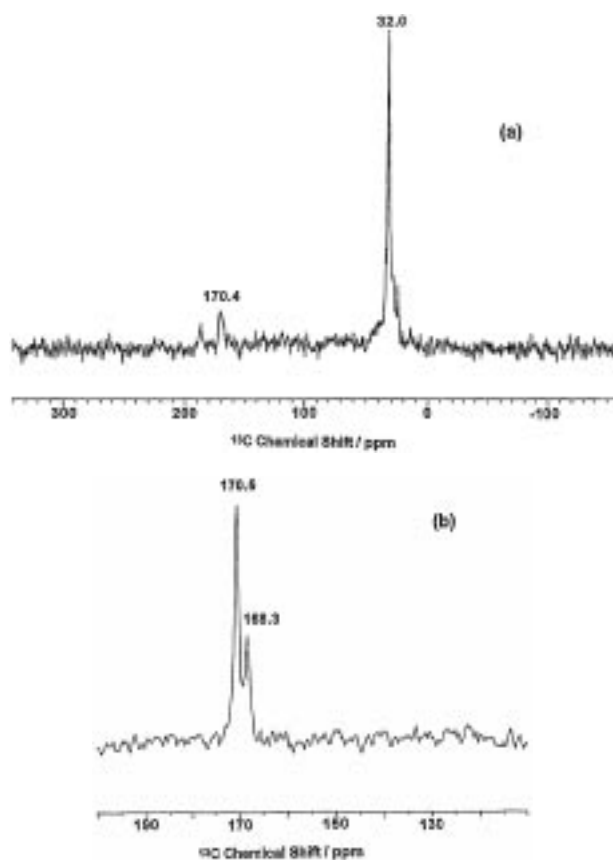


Figure 10 Solid state  $^{13}\text{C}$  MAS NMR spectra of (a) hypochlorite-treated bovine bone matrix and (b) commercial sample of calcium carbonate.

the extent of binding energy shifts or “charging.” Normally when elements other than carbon are being analyzed, the binding energy (284.8 eV) of C 1s from adsorbed “adventitious” hydrocarbons (mostly from vacuum pump oil) is used as an internal charging reference. This is not possible in the case of the bone samples examined in the present study because the C 1s signal from the bone swamps the adventitious carbon component of the peak. Thus *comparisons* of overall C 1s narrow scan peak profile shapes were made from sample to sample to deduce changes in the bone after processing. The mode of interpretation adopted consisted of comparing overall C 1s narrow scan peak shapes of different bone specimens with that of dry rolled collagen foam and pure calcium carbonate and noting any differences.

#### 4.5.2. XPS of dry collagen foam

Fig. 11(a) is the C 1s narrow scan of a slab of collagen foam material extracted from cattle hide. The profile can be deconvoluted into three synthetic profiles centered at the (uncorrected) binding energy positions of 287.7, 288.9 and 291.1 eV. There are few papers dealing with XPS studies of collagen surfaces in the literature. Radu and Baiulescu [39] report a narrow scan C 1s spectrum of a collagen membrane surface. Their observed C 1s profile was broad and complex and was deconvoluted into four peaks. They attributed these deconvoluted C 1s peaks to various functional groups in the collagen structure, *viz.*,  $-\text{CO}_2$  and  $\text{N}=\text{C}=\text{O}$  groups in collagen (at highest binding energy),  $\text{C}=\text{O}$ ,  $\text{O}-\text{C}-\text{O}$ ,  $\text{C}-\text{O}$ , and  $\text{C}-\text{N}$  carbons (intermediate binding energy) and aliphatic type carbons ( $\text{CH}_2$ ,  $\text{CH}_3$ ) (lowest binding energy). In the

absence of a more comprehensive study on collagen, the assignment of the deconvoluted C 1s peaks in the present study could be similarly assigned as in [39].

#### 4.5.3. XPS of various bone matrix samples

Bone matrices and crushed bone powders from different animal species after pressure cooking, solvent extraction and deproteination examined all gave complex narrow scan C 1s spectra profiles which, despite the variability between the samples, essentially showed two “types” of profiles. The first type was the “collagen and residual fat” type profile (Fig. 11(a) and (b)), and the second the “calcium carbonate” type profile (Fig. 12(a) and (b)).

#### 4.5.4. The “collagen and residual fat C 1s narrow scan” profile

Fig. 11(b) represents a C 1s narrow scan of a sample of milled bovine bone. Comparison of this C 1s narrow scan profile with the typical profile for collagen (Fig. 11(a)) shows the two are somewhat similar, *i.e.* the predominant contributor to the observed C 1s profile is the collagen contained in the crushed bovine bone. The major difference in the profiles is the appearance of a weak feature at *ca.* 285.3 eV (charge uncorrected). As the milled bovine bone did not have an additional wash in organic solvent to remove residual traces of surface-adsorbed fat (*cf.* the bovine cubes which were refluxed in methyl acetate) it is likely that the 285.3 eV peak is due to residual surface fat. XPS spectra of a bone cube microwaved in water and then IPA showed a collagen-type profile *without* the 285.3 eV peak thus confirming

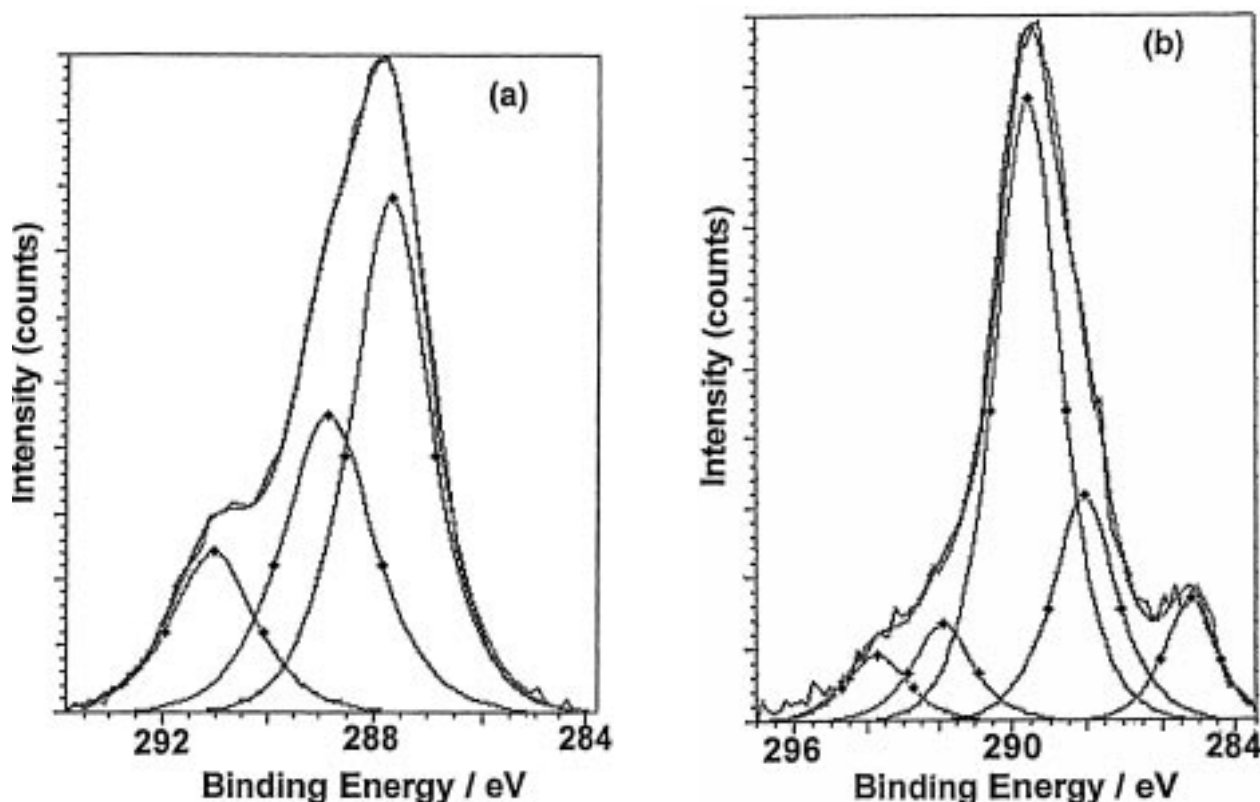


Figure 11 C 1s X-ray photoelectron narrow scan of (a) dry collagen foam and (b) milled bovine bone.

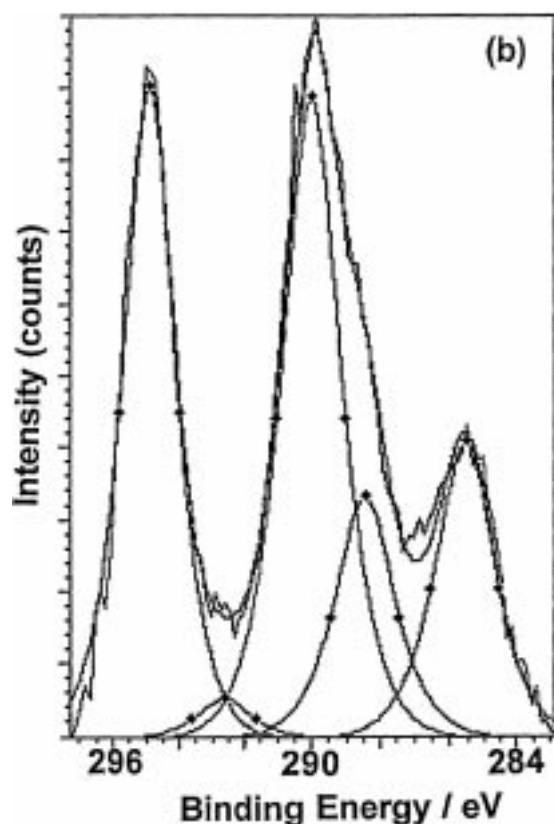
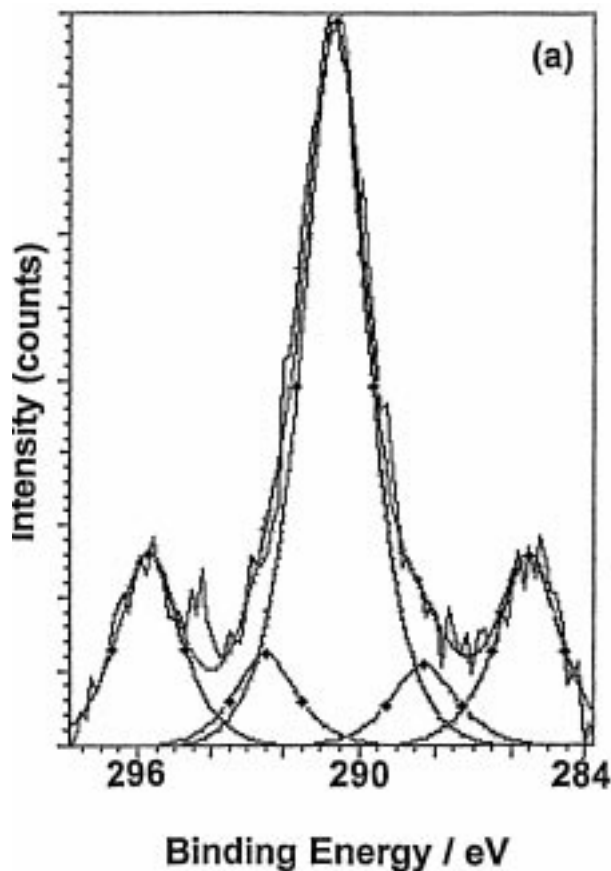


Figure 12 C1s X-ray photoelectron narrow scan of (a) defatted/hypochlorite-treated bovine bone and (b) commercial calcium carbonate.

this assignment. XPS spectra from milled bone powders from other animal species, such as deer and sheep, gave similar C 1s narrow scan profiles which also featured a

C 1s peak due to residual fat. The observation of such peaks in the XPS was supported by FTIR spectra of the bone materials which indicated the presence of fat. XPS of a sample of "Kiel Bone" obtained for the study gave very similar spectra, i.e. a collagen and residual fat C 1s profile was observed.

#### 4.5.5. The "calcium carbonate" type C 1s narrow scan profile

Fig. 12(a) is a C 1s narrow scan profile of deproteinated bovine bone cubes (by hypochlorite treatment). Instead of the asymmetric and complex "collagen" type profile, a simpler C 1s profile centered at 290–291 eV (uncorrected for charging), flanked by two weak peaks at 285.6 eV and 295.7 eV, is observed. Observed C 1s profiles of this type are referred to as "calcium carbonate-type" profiles because of their similarity (in part) to the C 1s narrow scan observed for a sample of pure calcium carbonate (Fig. 12(b)). In the case of the deproteinated bone, the carbonate-type C 1s profile is due to hydroxycarbonate apatite remaining in the bone in its original architecture. This mineral carbonate component may well have been coated with collagen in bone samples prior to deproteination and was hence not observable on the surface of such samples. Given the mineral matrix of the deproteinated bone is (like calcium carbonate powder) electrically insulating, a large degree of sample charging is expected which causes large binding energy shifts for C 1s in the observed narrow scans of the samples. The 295.7 eV peak in Fig. 12(a) can be assigned to carbonate in hydroxycarbonate apatite (Fig. 12(b)) while the 290–291 eV peak is probably due to adventitious hydrocarbons (which if used an internal charging reference would indicate a charging shift of +6.2 eV for all peaks in the spectrum). The origin of the 285.6 eV peak is unknown. It is possibly a spectral artefact species caused by the X-ray induced reduction of carbonate. It is obvious that the analysis of complex natural materials like bone requires care in its interpretation. The use of standards other than adventitious carbon is recommended in order to provide a more reliable means of assessing charging.

## 5. Conclusions

In general, it has been shown that abattoir-sourced bovine cancellous bone can be successfully converted by a process of boiling, solvent treatment and deproteination to a modifiable implant material for biomedical purposes. The end product of the bone processing is a shapeable calcium hydroxycarbonate matrix in which the original porous architecture of the bone is retained so rendering it valuable for any custom surgical applications in which tissue ingrowth is an important part of the implant integration process in the body. The changes in the bone's physical properties can be monitored facily by various spectroscopic, microscopic and chemical analysis techniques so allowing good control of the simple processing steps employed.

## Acknowledgments

The New Zealand Foundation for Research, Science and Technology (FRST) is acknowledged for funding granted to this project from the Public Good Science Funding Round. Waitaki Biosciences in Christchurch, New Zealand is also thanked for use of supercritical CO<sub>2</sub> fluid extraction facilities. G.S.J. is grateful to MIRINZ Food and Technology Research Limited for an annual scholarship to carry out the research. We are also grateful to Drs Richard Havercamp (University of Auckland), Roger Mederr (Forestry Research Limited Rotorua) and Nick Kim (University of Waikato) for advice in the use of or for recording spectra on XPS, solid state NMR, DSC and AAS instrumentation. We would also like to acknowledge the assistance of Mrs Wendy Jackson for recording some of the scanning electron micrographs.

## References

1. A. JOBLING and C. A. JOBLING, Proceedings of the Easter School in Agricultural Science, University of Nottingham, **36** (London, Butterworths, 1983) pp. 183.
2. T. AKAZAWA and K. KODAIRA, *Phosphorus Res. Bull.* **1** (1991) 215.
3. P. FRAYSSINET, E. ASIMUS, A. AUTEFAGE and J. FAGES, *J. Mater. Sci.: Mater. Med.* **6** (1995) 473.
4. D. CHAPPARD, C. FRESSONNET, C. GENTY, M.-F. BASLE and A. REBEL, *Biomaterials* **14** (1993) 507.
5. C. REY, M. SHIMIZU, B. COLLINS and M. J. GLIMCHER, *Calcif. Tiss. Int.* **49** (1991) 383.
6. *Idem.*, *ibid.* **46** (1990) 384.
7. C. REY, B. COLLINS, T. GOEHL, I. R. DICKSON and M. J. GLIMCHER, *ibid.* **45** (1989) 157.
8. M. A. WALTERS, Y. C. LEUNG, N. C. BLUMENTHAL, R. Z. LEGEROS and K. A. KONSKER, *J. Inorg. Biochem.* **39** (1990) 193.
9. M. A. WALTERS, N. C. BLUMENTHAL, Y. LEUNG, Y. WANG, J. L. RICCI and J. M. SPIVAK, *Calcif. Tiss. Int.* **48** (1991) 368.
10. I. REHMAN, R. SMITH, L. L. HENCH and W. BONFIELD, *J. Biomed. Mater. Res.* **29** (1995) 1287.
11. A. BERTOLUZZA, C. FAGNANO, A. TINTI, M. A. MORELLI, M. R. TOSI, G. MAGGI and P. G. MARCHETTI, *J. Raman Spectrosc.* **25** (1994) 109.
12. G. R. SAUER, W. B. ZUNIC, J. R. DURIG and R. E. WUTHIER, *Calcif. Tiss. Int.* **54** (1994) 414.
13. Y. LEUNG, M. A. WALTERS, N. C. BLUMENTHAL, J. L. RICCI and J. M. SPIVAK, *J. Biomed. Mater. Res.* **29** (1995) 591.
14. L. SAVARINO, S. STEA, D. GRANCHI, M. E. DONATI, M. CERVELLATI, A. MORONI, G. PAGANETTO and A. PIZZOFERRATO, *J. Mater. Sci.: Mater. Med.* **9** (1998) 109.
15. S. KANO, A. YAMAZAKI, R. OTSUKA, M. OHGAKI, S. NAKAMURA, M. AKAO and H. AOKI, Proceedings of the First International Symposium on Apatite, Mishima, Japan, July 1991 (Japanese Association of Apatite Science, March, 1992) 91.
16. W. P. AUE, A. H. ROUFOSSE, M. J. GLIMCHER and R. G. GRIFFIN, *Biochemistry* **23** (1984) 6110.
17. J. R. MOORE, L. GARRIDO and J. L. ACKERMAN, *MRM* **33** (1995) 293.
18. New Zealand MAF MQM Manuals, MQM12 Overseas Requirements and Certification, Volume 2 (updated continually).
19. AOAC International 16th edition (Association of Official Analytical Chemists) **2** (1995) p. 7.
20. W. R. WALSH, M. OHNO and N. GUZELSU, *J. Mater. Sci.: Mater. Med.* **5** (1994) 72.
21. J. E. SWAN and P. J. TORLEY, MIRINZ Report 883, ISSN 0465-4390, August, 1991.
22. D. J. SHARP, K. E. TANNER and W. BONFIELD, *J. Biomechanics* **23** (1990) 853.
23. D. M. P. MINGOS and D. R. BAGHURST, *Chem. Soc. Rev.* **20** (1991) 12.
24. K. GANZLER, A. SALGO and K. VALCO, *J. Chromatography* **371** (1986) 299.
25. W. T. CUNNINGHAM and A. Y. BALEKJIAN, *Oral Surgery* **49** (1980) 175.
26. M. OTTER, S. GOHEEN and S. W. WILLIAMS, *J. Orthopaedic Res.* **6** (1988) 346.
27. K. HASEGAWA, C. H. TURNER and D. B. BURR, *Calcif. Tiss. Int.* **55** (1994) 381.
28. J. J. BROZ, S. J. SIMSKE, W. D. CORLEY and A. R. GREENBURG, *J. Mater. Sci.: Mater. Med.* **8** (1997) 395.
29. J. J. KLAWITTER and S. F. HULBERT, *J. Biomed. Mater. Symp.* **2** (1971) 161.
30. W. I. ABDEL-FATTAH and F. A. NOUR, *Thermochim. Acta* **218** (1993) 465.
31. M. D. GRYNPAS, K. P. H. PRITZKER and R. G. V. HANCOCK, *Biolog. Trace Element Res.* **13** (1987) 333.
32. H. BEM and D. E. RYAN, *Anal. Chim. Acta* **135** (1982) 129.
33. Y. GELINAS, M. YOULA, R. BELIVEAU and J.-P. SCHMIDT, *ibid.* **269** (1992) 115.
34. J. C. ELLIOT, in "Structure and chemistry of the apatites and other Calcium orthophosphates", Studies in Inorganic Chemistry **18** (Elsevier, London, 1994) 229.
35. K. BESHAH, C. REY, M. J. GLIMCHER, M. SCHMIZU and R. G. GRIFFIN, *J. Solid State Chem.* **84** (1990) 71.
36. N. L. CRAIG and D. M. HERCULES, *Analytical Lett.* **8** (1975) 831.
37. D. M. HERCULES and N. L. CRAIG, *J. Dent. Res.* **55** (1976) 829.
38. W. J. LANDIS, M. D. GRYNPAS, R. M. LATANISION and J. R. MARTIN, *Microbeam Analysis* (1982) 121.
39. G.-L. RADU and G. L. BAIULESCU, *J. Molec. Struct.* **293** (1993) 265.

Received 13 November 1998  
and accepted 24 August 1999